http://doi.org/10.29227/IM-2021-02-09 Received: 08 Jun 2021, Accepted: 06 Aug 2021, Published: 10 Nov 2021

Rule-based Classification of Airborne Laser Scanner Data for Automatic Extraction of 3D Objects in the Urban Area

BUI Ngoc Quy[1, *], LE Dinh Hien[1, 2], DUONG Anh Quan[1], NGUYEN Quoc Long[1]

[1] Hanoi University of Mining and Geology, 18 Vien street, Hanoi, Vietnam

[2] Natural resources and Environment one member co., ltd, Hanoi, Vietnam

Corresponding author: buingocquy@humg.edu.vn

Abstract. LiDAR technology has been widely adopted as a proper method for land cover classification. Recently with the development of technology, LiDAR systems can now capture high-resolution multispectral bands images with high-density LiDAR point cloud simultaneously. Therefore, it opens new opportunities for more precise automatic land-use classification methods by utilizing LiDAR data. This article introduces a combining technique of point cloud classification algorithms. The algorithms include ground detection, building detection, and close point classification - the classification is based on point clouds' attributes. The main attributes are heigh, intensity, and NDVI index calculated from 4 bands of colors extracted from multispectral images for each point. Data of the Leica City Mapper LiDAR system in an area of 80 ha in Quang Xuong town, Thanh Hoa province, Vietnam was used to deploy the classification. The data is classified into eight different types of land use consist of asphalt road, other ground, low vegetation, medium vegetation, high vegetation, building, water, and other objects. The classification workflow was implemented in the TerraSolid suite, with the result of the automation process came out with 97% overall accuracy of classification points. The classified point cloud is used in a workflow to create a 3D city model LoD2 (Level of Detail) afterward.

Keywords: Point cloud, Lidar data, NDVI index, Classification algorithms, 3D city

1. Introduction

Delivering precise and timely data is always an indispensable factor for the management, planning, and landscape pattern analysis of urban land. Recently, alongside satellite images and UAV (Unmanned Aerial Vehicle) data, airborne LiDAR (Light Detection and Ranging) has been widely used as an effective data collection method that helps to produce fast, large scale and accurate geospatial data., it shows the flexibility in flying shooting and data acquisition for small and medium-sized areas. The UAV With UAV technology image data can be used to create digital elevation models (DEM) [1], create 3D map models [2, 3], etc. In addition, point cloud data is processed from UAV images are also classified to create 3D models for terrain objects, especially for open-pit mines [4]. Meanwhile, aviation LiDAR technology shows the ability to fly and capture data in a wide range and is widely used in studies of the earth's surface. In the earliest period, nDSM (normalized Digital Surface Model) extracted from LiDAR data has been used as a criterion for urban land classification [8]. Besides, there were several studies about LiDAR intensity not only for depicting the natural surface condition such as surface moisture [9], flow recognition and aging of lava [10], wetland hydrology [11], and rock properties [12] but also supporting in municipal area cover classification. LiDAR intensity was first utilized by Song, J.H and et al in 2002 [13]; the intensity value of asphalt road, grass, house roof, and the tree was inspected to have an adequate difference for land cover classification. However, using intensity data as a standalone factor was asserted about its limitation in various research [13-18]. Thus, there was plenty of research that integrates LiDAR intensity with height value to eliminate that limitation such as Charaniya, A. et al, 2004 [8] use intensity to separate road from low vegetation, Brennan in 2006 [15] sort out structures with the same height by the intensity and many others [19-22]. Alongside intensity, RGB (Red Green Blue) satellite images and onboard aerial images with direct geo-referencing have also been combined with LiDAR height data for land cover classification [8, 14, 22-28]. Normalized difference vegetation index (NDVI) is another essential factor for land use classification; the adoption of NDVI with LiDAR data has been implemented in various studies [21, 22, 27, 29, 30] that help to raise the efficiency of the classification enormously. Thus, it can be seen that NDVI value from images and the Intensity value of LiDAR data are both good elements to be used in classification. Currently, the use of NDVI and Intensity combination is utilized in land cover classification [31], therefore, if the combination can be used to classify point cloud, it can facilitate the further use of point cloud such as for making 3D city model purpose. This study introduces a method of combining both intensity value of LiDAR data and NDVI, which extracted from onboard high-resolution images with

different LiDAR point cloud classification algorithms in consist of ground detection routine, classification by height compared to ground, building detection routine, and classification by close point and afterward, the classified point cloud is used as material to build a LoD2 city model. The method will help build an automatic classification workflow for LiDAR point cloud into eight different land-use types, including asphalt road, other ground, low vegetation, medium vegetation, high vegetation, building, water, and other objects. TerraSolid suite was used to perform the automation process. The result came out with 97% overall of points were correctly classified. Besides, another workflow to automatically create a 3D city model is also introduced in this study to provide a LoD2 city model which can be used for various applications.

2. Data acquisition and study area

2.1. Lidar system: City Mapper

The LiDAR system used is CityMapper of Leica Geosystem (Fig. 1). It consists of a 0.9 nm wavelength LiDAR scanner, an 80 mm focal length multispectral camera, and integrated with GNSS and IMU system, which provide high accuracy of 5 cm horizontal and 10 cm vertical. The data was captured at 1200 m height with an average point density of 5 pts/m^2 and 7 cm GSD images. It took 3 flight trips (2 North-South lines and 1 crossed line) to cover the study area in sunny weather. The trajectory was processed in Inertial Explorer, images, and point clouds were processed in HxMap.

Fig. 1. Leica City Mapper system.

2.2. Study area

The chosen study zone is 80 hectares in Quang Xuong town, Thanh Hoa province, Vietnam. It is a plain area located in 19°44’04’’ N, 105°46’53’’ E with around 5 meters above sea level height (Fig. 2). We select this area because it has enough of 8 land use objects, including asphalt road, other ground, low vegetation, medium vegetation, high vegetation, building, water, and other objects (traffic signs, traffic lights, trash cans, cars, etc.).

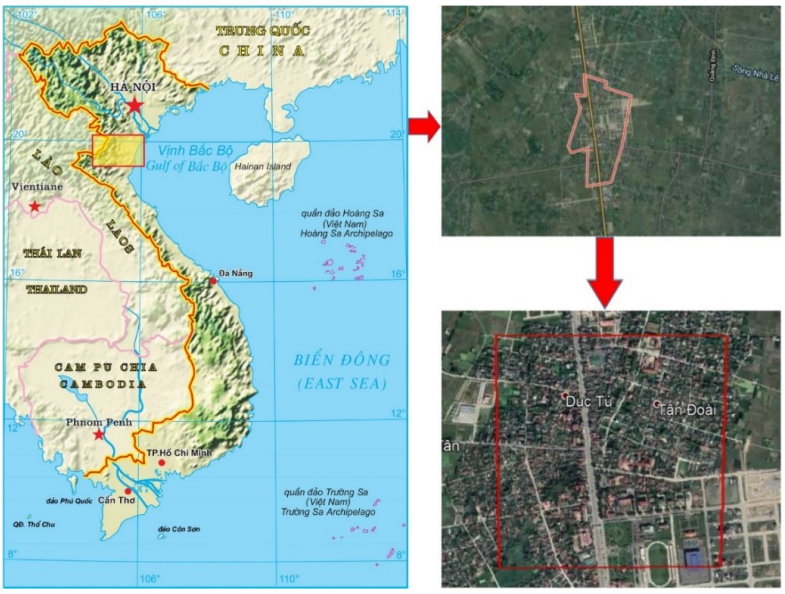

Fig. 2. Area of study.

3. Methodology

3.1. Workflow and classification threshold

Workflow: The point clouds of the study area were taken by using the Airborne Lidar system. The lidar signals and images go through the pre-processing with rectification and GCPs adjustment. We used HxMap which is a Leica software to process Leica City Mapper's data to export the LiDAR point clouds with four bands of color, including Red - Green - Blue - Near Infrared. Based on the point cloud characteristics, we apply the automatic classification process to have point clouds in different classes. The classified point cloud is used in a City 3D modeling workflow to build a LoD2 City Model. The detailed workflow is described in the following Figure 3.

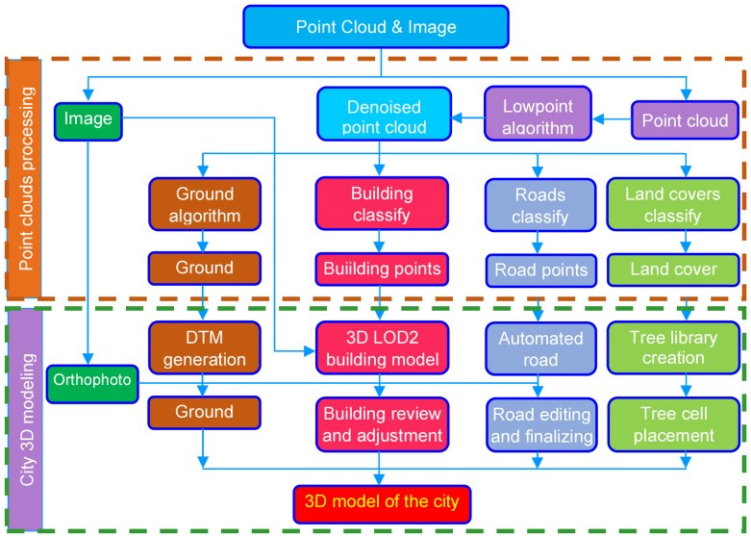

Fig. 3. Point clouds classification & City 3D modeling workflow.

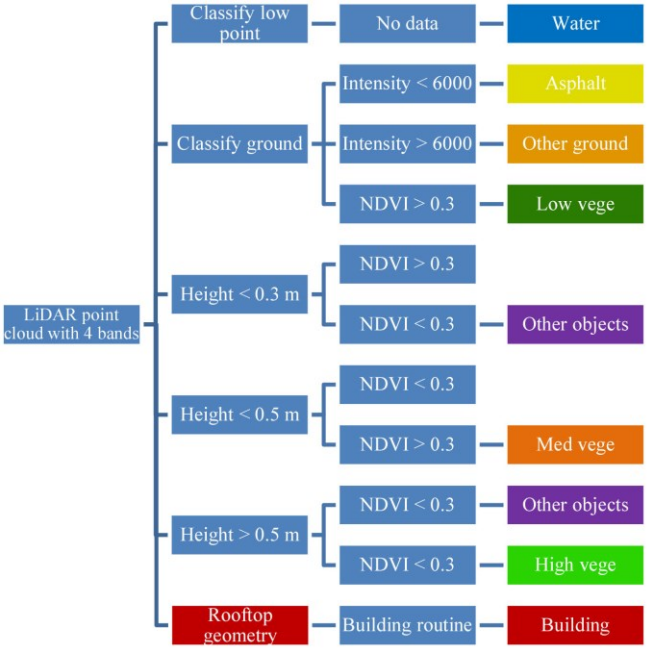

Fig. 4. Classification threshold.

Classification threshold for point clouds: Figure 3 described the overview of the 3D model building workflow. Inside this workflow, the first step is the classification of points in the point clouds to 8 classes. The classification is based on the thresholding levels described in Figure 4.

The threshold level developed base on natural characteristics of object classes in point clouds. There are four characteristics used to develop the threshold level: Intensity, NDVI, Height, and Geometry.

3.1.1. Intensity

Intensity is the ratio of the strength of reflected light to that of emitted light, and the reflectance of the reflecting object has the most impact on its value. Reflectance is different between different material attributes as well as the light used. Therefore, intensity can be used to differentiate point clouds (Fig. 5). We proceeded to manually collect sample intensity values for Asphalt, Concrete, Tile, Soil Lane, and soil to have a table for intensity range below (Tab. 1):

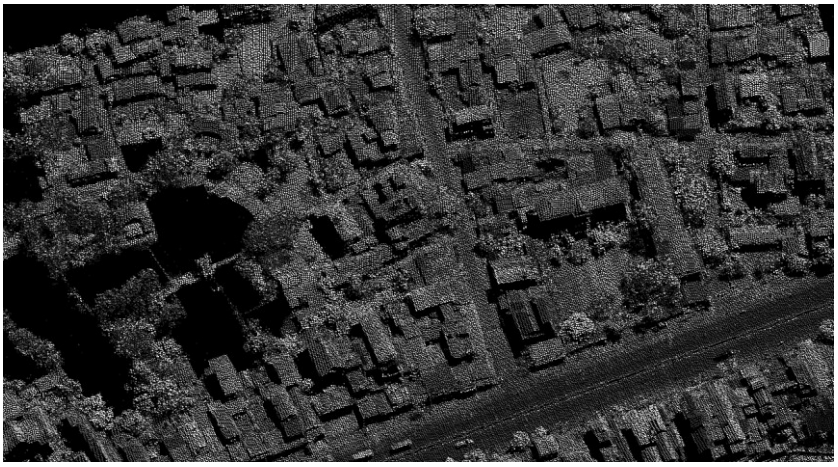

Fig. 5. Point cloud in the display of intensity.

Tab. 1. Intensity range of CityMapper point clouds for different objects.

Order	Objects	Intensity range	Order	Objects	Intensity range
1	Asphalt	2100-5400	3	Tile	7300-9700
2	Concrete	9000-12500	4	Soil lane, soil	7500-13600

From this table, it can be seen that Asphalt can be filtered out from other ground objects by intensity value. Because the flat ground in the area consists of Asphalt, concrete, tile, soil lane, soil.

3.1.2. NDVI

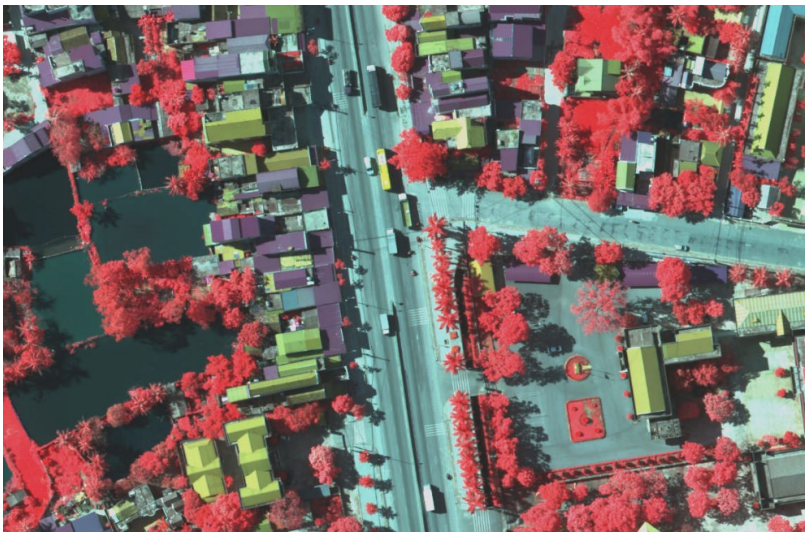

Fig. 6. The area display in the color infrared image.

The NDVI of the CityMapper is calculated by the following formula:

$$\mathrm{NDVI} = \frac{(\mathrm{NIR} - \mathrm{Red})}{(\mathrm{NIR} + \mathrm{RED})}$$

By design, the NDVI itself thus varies between -1.0 and +1.0. Most of the collected vegetation points

samples have the value of intensity above 0.3 since the capture data date is in summer and all kinds of plants here have green leaves. Figure 6 described the point cloud of the study area display in the color infrared image.

3.1.3. The height of points

The height of points is the different elevation of points compared to the ground surface. It is an essential factor to separate different types of objects. For instance, the grass is below 0.3 m in height, while plant pots & bushes range from 0.3 m to 0.5 m and trees are above 0.5 m.

3.1.4. Geometry of points group

A group of points has its geometry; it may present a planar, a curve, or irregular shapes. Based on the shapes, the object can be detected automatically. For example, the rooftop may have planar shapes, and the tree may have irregular shapes (Fig .7).

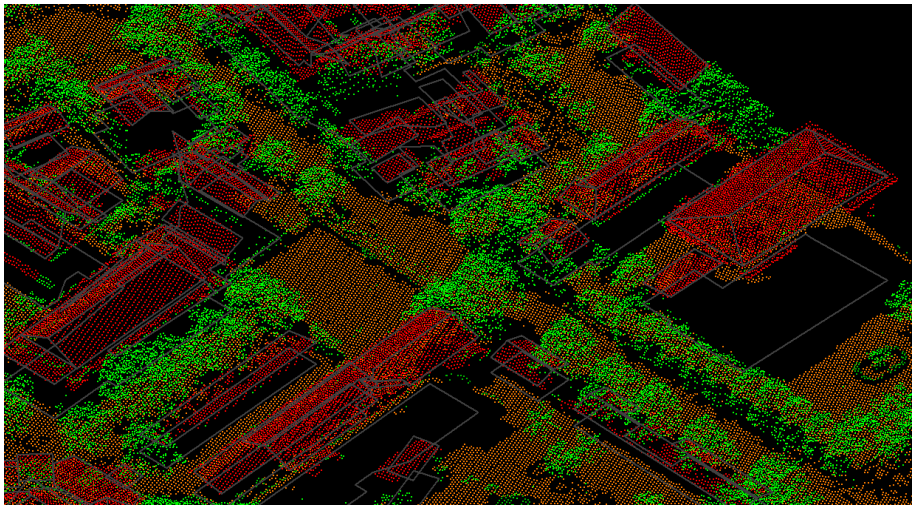

Fig. 7. Rooftop geometry.

3.2. Classification processing

3.2.1 Classify low, isolated point/water

The low-point routine which is used to denoise the point cloud classifies single points or groups of lower points than other points in the surrounding. There might be possible error points that are clearly below the ground. The elevation value of each point or point group with any other point within a given 2D radius will be collated. The routine will classify the point or point group to a low point group if it is lower than any other point.

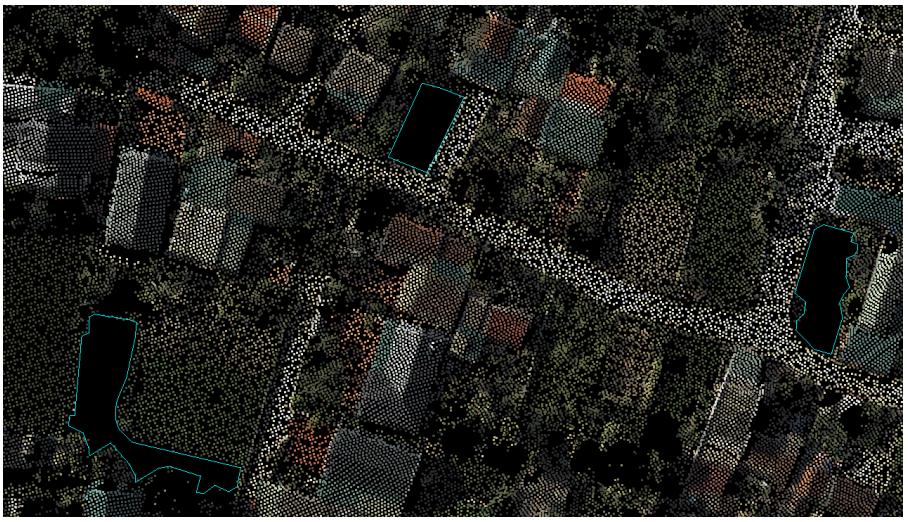

Fig. 8. Water area.

Next, isolated noise points in the air or on the ground will be filtered out by an isolated routine. The loop detects points with fewer neighbor points within a 3D search radius than defined in the routine's settings.

After the low point and isolate routine, an automatic drawing polygon routine will be used to draw boundaries for no data areas for marking as water land use (Fig. 8). The remaining points are ready for the following ground routine.

3.2.2. Classify ground

The classify ground routine automatically searches ground LiDAR points by making a triangulated surface model iteratively. The loop begins by selecting the lowest point with a potential ground surface nearby. Afterward, it makes a surface model (TIN) from the starting point. The model becomes more closely to the proper ground surface by each added point.

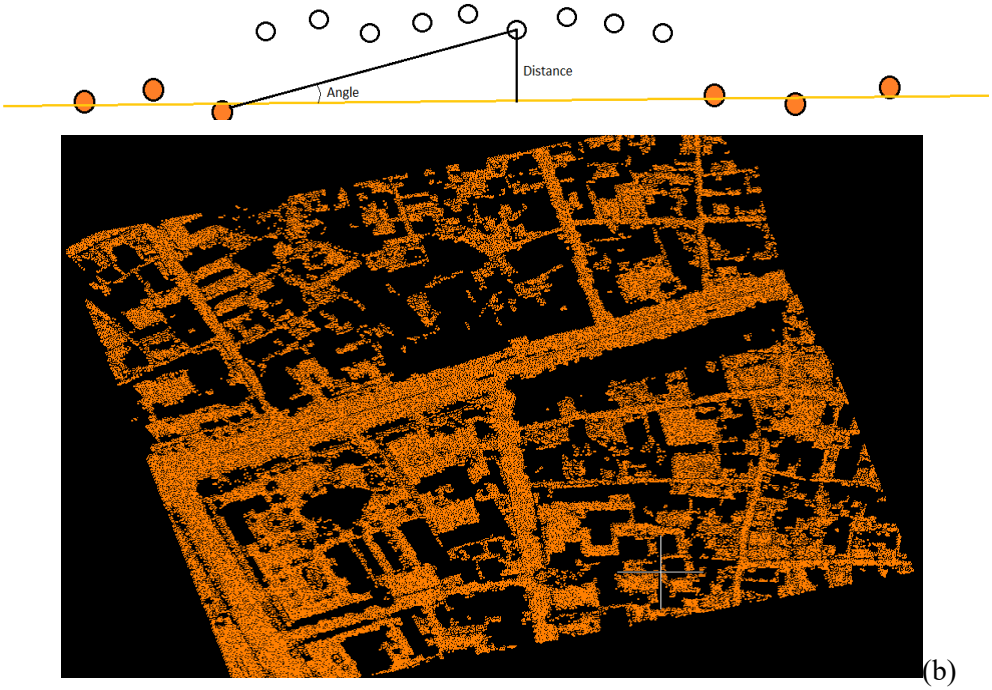

Fig. 9. The ground routine and Ground point.

The chosen algorithm uses parameters of iteration angle and iteration distance (Fig. 9a). Iteration angle is the maximum angle between the line of the ground surface made by two ground points at a far distance and the line which connects the ground point to the search point. Iteration distance ranges from the search point projected in the nadir direction to the ground surface. It helps to prevent detecting points that are too high from the ground.

After this ground routine, a group of ground points was detected (Fig. 9b), then, with the NDVI routine for each point NDVI value >0.3, mixed in vegetation points will be filtered out. Finally, with the intensity routine, asphalt road points will be classified with an intensity value lower than 6000, and the rest will go to other ground points.

3.2.3. Classify vegetation

Before the vegetation routine, we use a macro to calculate the distance of all remaining points to the ground class. Then, a height algorithm is utilized to classify three types of vegetation.

All points with a height value below 0.3 m go to low vegetation.

Points with a height value below 0.5 m go-to medium vegetation.

Points with a height value above 0.5 m go to high vegetation.

Finally, an NDVI routine will be used to filter out other objects from vegetation that have an NDVI value < 0.3

3.2.4. Building routine

The building routine detects points on houses' roofs with a flat distribution from other objects' classes. Holes above the ground class will begin to search for points on planar surfaces first. Minimum acreage and roof thickness of houses need to be set as parameters used for the routine.

Afterward, a close point routine will be applied to bring roof structure from other objects class to building class. The loop looks for nearby points with a set 3D distance compared to the current building class.

3.3. 3D city model

3.3.1. True Orthophoto generation.

The True Orthophoto is created from the Aerial Images (Fig. 10). After a triangulation process, the external orientation of each image is refined to have better accuracy. The Lidar point cloud is used to generate the DSM of the study area. All of the images will be projected to the DSM to form a True Orthophoto of the area.

Fig. 10. Orthophoto of the study area.

3.3.2. DTM generation & textured ground model

DTM is generated as a TIN (Triangulated Irregular Network) model with the input from the ground point layer (Fig. 11). After that, the TIN model will be texturized using the True Orthophoto from the base ground model for the 3D city model.

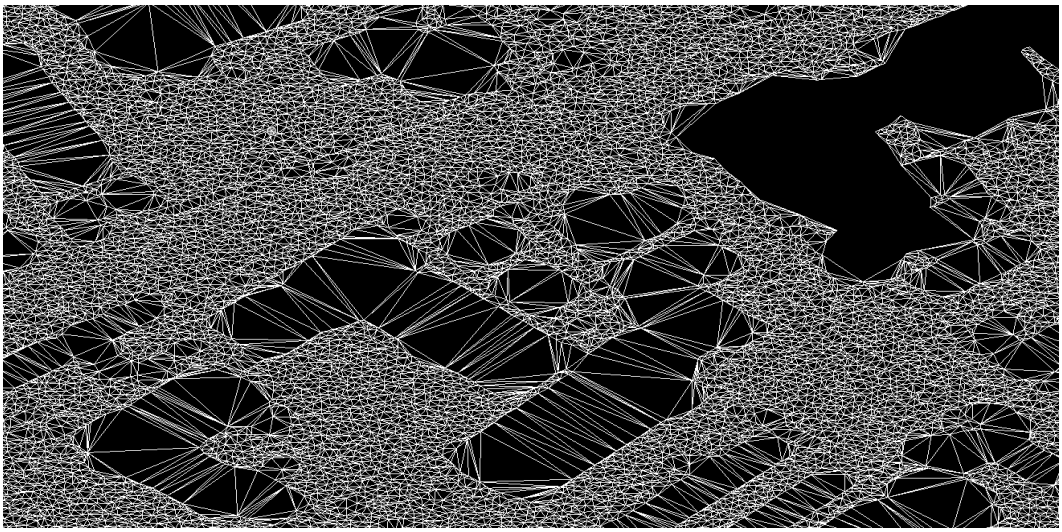

Fig. 11. TIN model.

3.3.3. Building model

The building point cloud layer is the input for this process. An algorithm is used to vectorize buildings automatically. After the automation, every shape of the buildings is checked with manual work. The building models are in the form of LoD2 (Fig. 12) and are texturized by cutting images from the True Orthophoto.

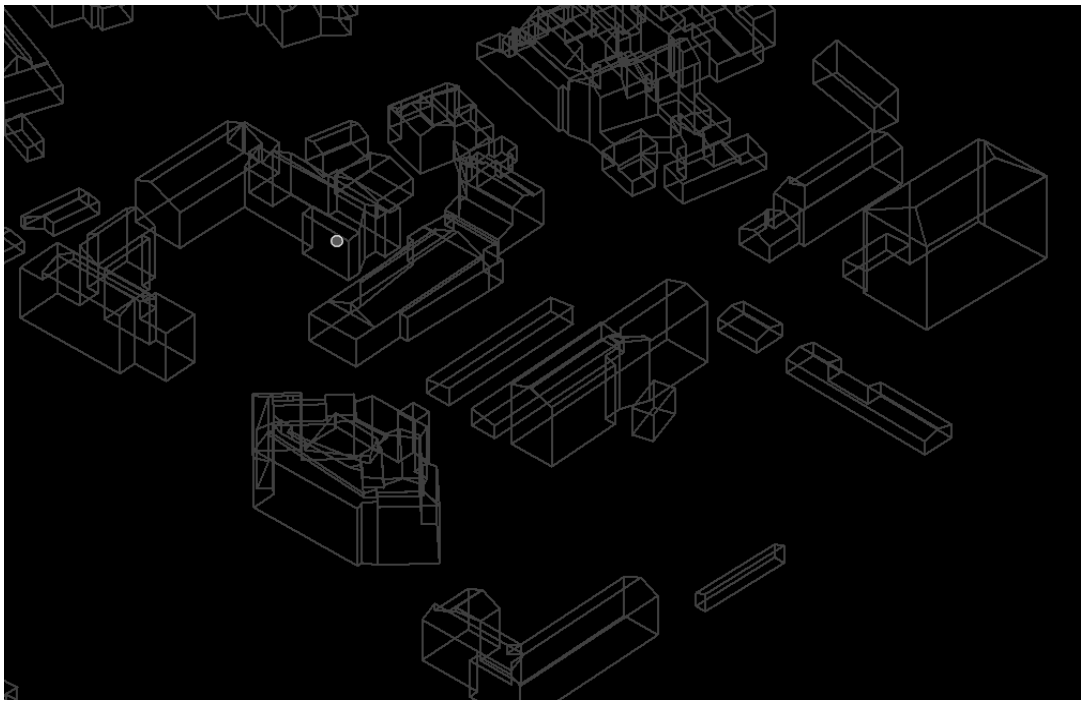

Fig. 12. Buildings models.

3.3.4. The road network

The road network is automatically vectorized by an algorithm with the input of the point cloud from the asphalt class. The road digitation is also checked with a manual process until acceptance.

3.3.5. The tree models

This process requires making a library of trees based on the shape and size of each type of tree (Fig. 13). Three vegetation layers are used as the input, each type of tree is viewed in a vertical section to draw the standard shape and define the parameters of size. A tree model is used correspondingly to each kind.

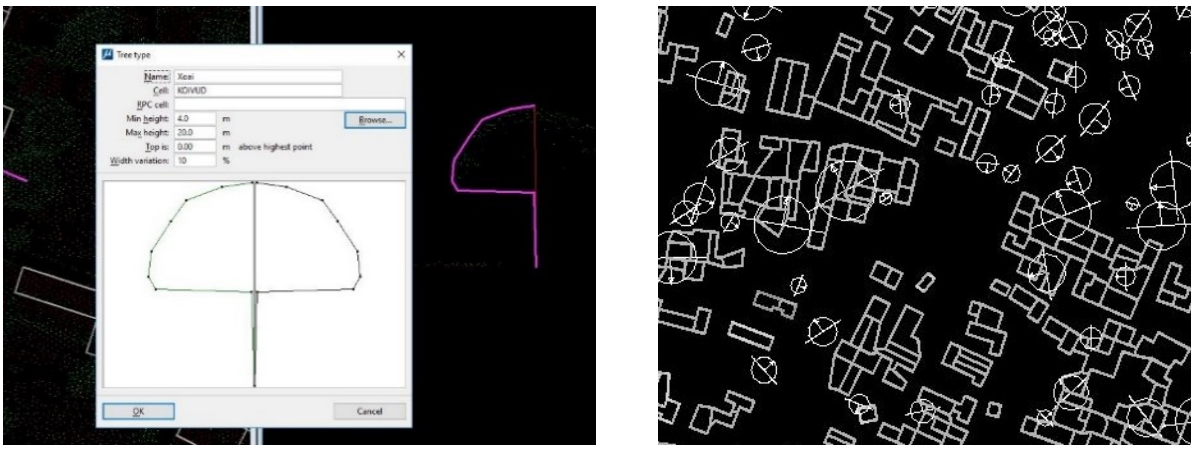

Fig. 13. Trees model.

Afterward, an automatic process is run to sift through the vegetation layer to detect trees. Correspond to each tree, a 3D tree cell from the library is placed on the model. Each tree cell will be present with a tree model from the library, respectively.

4. Result and discussion

4.1. Result

4.1.1. Point cloud classification

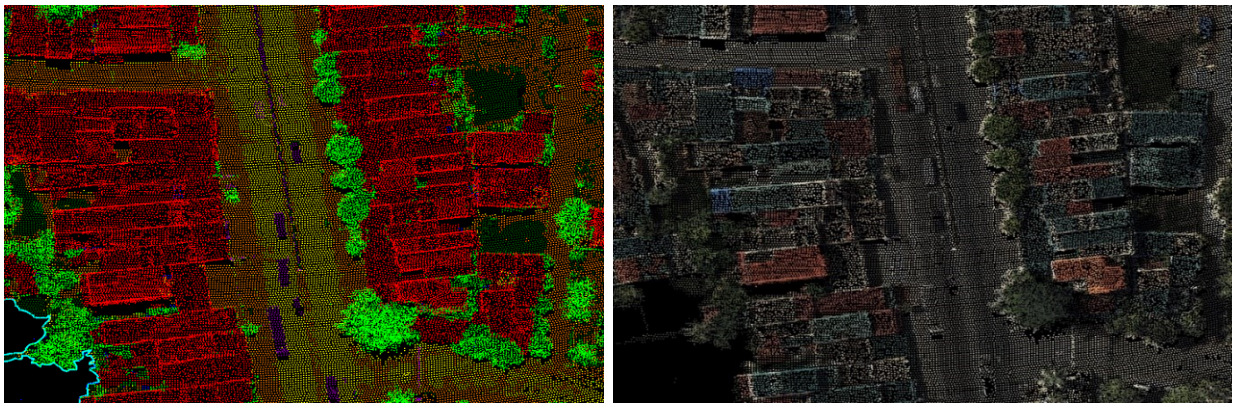

(a) (b)

Fig. 14. LiDAR point clouds of Quang Xuong town after the automatic classification process. (a) Point clouds view by class; (b) Point clouds view by color.

After processing through the workflow, the LiDAR point clouds of the study area were automatically classified into seven different classes (Fig. 14): asphalt road, other ground, low vegetation, medium vegetation, high vegetation, building, and other objects (water areas were vectorized as polygons). A manual checking process was performed afterward with the help of referenced orthophoto to collect incorrect classified points.

The result came out with a very promising overall accuracy of 97.18 % as an average value of classification precision of 7 classes totaled up in Table 2.

Tab. 2. Classification accuracy of 7 classes.

	Asphalt	**Other ground**	**Low vegetation**	**Medium vegetation**	**High vegetation**	**Building**	**Other Objects**
Incorrect classified points	s	9637	12519	7398	42361	26521	19841
Total points	169647	745522	600895	234237	1091304	1048832	400823
Accuracy (%)	98.18	98.71	97.92	96.84	96.11	97.47	95.05

The highest accuracy belongs to other ground and asphalt classes (98.71% and 98.18%). It shows that the ground routine worked practically effectively. The intensity value helped filter out asphalt quite thoroughly, thanks to the assistant of NDVI, because most of the low vegetation points were classified as ground points after the ground routine. It has an intensity range quite similar to asphalt. Other objects class has the lowest accuracy due to the complexness of the roof structure of houses in town. NDVI value helps filter vegetation, but the accuracy peaked at 97.92% for low vegetation.

4.1.2. 3D city model

The 3D city model of the study area (Fig. 15) is the combination of 4 layers:

- The 3D textured ground model as the base ground layer
- The road networks drawing layer
- The tree models
- 3D LoD 2 building model

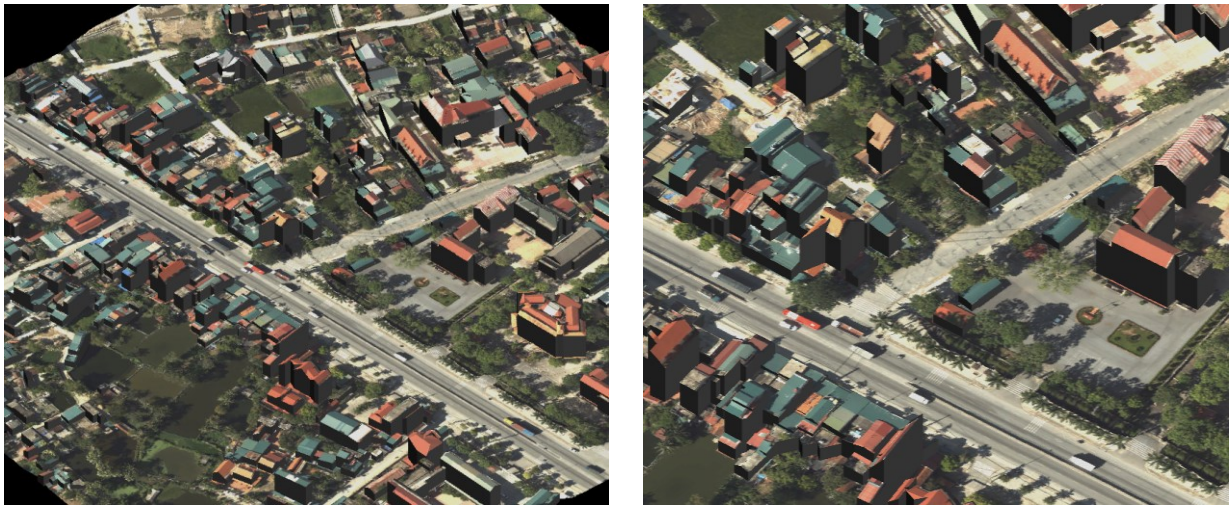

Fig. 15. 3D City model.

4.2. Discussion

The data is captured with the CityMapper with only one nadir camera (the full CityMapper has 4 more oblique cameras), thus, we do not have the oblique images to texture the facades. Therefore the building wall is not used in this research. It is classified into the point class of other objects.

The best setup for a city 3D model is capturing data at around 700-800 m AGL (above ground level) to have the best surface point cloud of the roof building. However, it is very difficult to ask for permission to fly below 1000 m above ground level in Vietnam, yet, the classification still can archive a high accuracy result and be able to create a LoD2 city model.

The outstanding feature of this method is the ability to classify high-density 3D point clouds with many points of different objects in a vertical direction, unlike other [14] that are required to convert LiDAR point clouds to a DTM or DSM surface. The automation process used in the study provides a high accuracy result (above 95% for all classes). With intensity and NDVI value, this method can filter out asphalt and vegetation together to classify up to 8 different classes. However, the data used in this study comes from the Airborne LiDAR system with an average point density of 5 pts/m^2 and unideal height condition, thus the detail of the point cloud for other objects is not enough to have further classification. Many different objects have to stay in one class - other objects. One suggestion could be the use of the combination data of airborne LiDAR with Mobile Mapping or other ground LiDAR stations to have a more detailed dataset to be able to develop a further classification for other objects. The asphalt and NDVI threshold in this project is localized, other researchers need to choose different values for different areas depending on the type of LiDAR sensors, materials, and trees.

5. Conclusion

This study introduces a method for automatic land use classification by combining many different point cloud routines with their innate value of intensity and NDVI from the onboard multispectral images. The conclusions are as follows.

First, it can be seen that the new airborne LiDAR system is capable of not only collecting data at high speed but also providing abundant and precise data for land use classification.

Second, the method helps eliminate the need for labor-intensive by building an automatic process that can exploit various characteristics of the point cloud to classify it with high accuracy (above 95% for all classes). With the help of onboard high-resolution multispectral images, we can wrap up the workflow by doing correctness by manually classifying the rest of the point cloud to deliver a complete classification.

Last but not least, the point cloud of the area after the classification process can be used to generate a 3D city model. The 3D model introduced in the study is the LoD2 model, which can be used for various purposes like city inventory for buildings, trees, etc.; city management and planning; handling emergencies; tourism, etc.

6. Acknowledgements

This study was supported by the Ministry of Education and Training Science project (N0. B2021-MDA-01), Vietnam.

7. References

1. Nguyen Quoc Long, Ropesh Goyal, Bui Khac Luyen, Le Van Canh, Cao Xuan Cuong, Pham Van Chung, Bui Ngoc Quy, Bui Xuan Nam, Influence of Flight Height on The Accuracy of UAV Derived Digital Elevation Model at Complex Terrain, Journal of the Polish Mineral Engineering Society, 1(45): 179 - 186, 2020. DOI: https://doi.org/10.29227/IM-2020-01-27.
2. Le Van Canh, Cao Xuan Cuong, Nguyen Quoc Long, Le Thi Thu Ha, Tran Trung Anh, Xuan-Nam Bui, 2020 – Experimental Investigation on the performance of RTK drones on 3D mapping Open-pit coal mines, Journal of the Polish Mineral Engineering Society, 2(46): 65–74. DOI: http://doi.org/10.29227/IM-2020-02-10.
3. Quy Ngoc Bui, Hiep Van Pham, Research on 3D model from unmanned aerial vehicle (UAV) images, Journal of Mining and Geology, 4(58): 1-11, 2017. http://tapchi.humg.edu.vn/vi/archives?article=873
4. Bui Ngoc Quy, Le Dinh Hien, Nguyen Quoc Long, Tong Si Son, Duong Anh Quan, Pham Van Hiep, Phan Thanh Hai, Pham Thi Lan, Method of defining the parameters for UAV point cloud classification algorithm, Journal of the Polish Mineral Engineering Society, 1(46): 49-56, 2020. DOI: https://doi.org/10.29227/IM-2020-02-08.
5. L. Q. Nguyen, 2021. Accuracy assessment of open-pit mine's digital surface models generated using photos captured by Unmanned Aerial Vehicles in the post-processing kinematic mode (in Vietnamese). Journal of Mining and Earth Sciences, Vol. 62, no. 4, Aug. 2021, p 38-47, doi:10.46326/JMES.2021.62(4).05.
6. Nguyen, Q. L., Le, T. T. H., Tong, S. S., Kim, T. T. H., (2020). UAV Photogrammetry-Based For Open Pit Coal Mine Large Scale Mapping, Case Studies In Cam Pha City, Vietnam. Sustainable Development of Mountain Territories, 12(4), 501-509. DOI: 10.21177/1998-4502-2020-12-4-501-509.
7. Nguyen Q. L., Ropesh G., Bui, K. L, Cao X. C., Le V. C., Nguyen Q. M., Xuan-Nam B., (2021). Optimal Choice of the Number of Ground Control Points for Developing Precise DSM using Light-Weight UAV in Small and Medium-Sized Open-Pit Mine. Archives of Mining Sciences, 66 (3), p 369-384, doi: 10.24425/ams.2021.138594.
8. Charaniya, A., Manduchi, R., Lodha, S., 2004. Supervised parametric classification of aerial LiDAR data. In: Proceedings of the IEEE 2004 Conference on Computer Vision and Pattern Recognition Workshop. Vol. 3. Baltimore, pp. 1–8.
9. Garroway, K., Hopkinson, C., Jamieson, R., 2011. Surface moisture and vegetation influences on LiDAR intensity data in an agricultural watershed. Canadian Journal of Remote Sensing 37(3): 275–284.
10. Mazzarini, F., Pareschi, M.T., Favalli, M., Isola, I., Tarquini, S., Boschi, E., 2007. Lava flow identification and aging by means of LiDAR intensity: Mount Etna case. Journal of Geophysical Research: Solid Earth 112 (B2)
11. Lang, M.W., McCarty, G.W., 2009. LiDAR intensity for improved detection of inundation below the forest canopy. Wetlands 29(4): 1166–1178.
12. Burton, D., Dunlap, D.B., Wood, L.J., Flaig, P.P., 2011. LiDAR intensity as a remote sensor of rock properties. Journal of Sedimentary Research 81(5): 339–347.
13. Song, J.H., Han, S.H., Yu, K.Y., Kim, Y.I., 2002. Assessing the possibility of land-cover classification using LiDAR intensity data. International Archives of the Photogrammetry, Remote Sensing and Spatial Information Sciences 34(Part 3/B): 259–262.

14. Minh, N.Q., Hien, L.P., 2011. Land cover classification using LiDAR intensity data and neural network. Journal of the Korean Society of Surveying, Geodesy, Photogrammetry and Cartography 29(4): 429–438.
15. Brennan, R., Webster, T., 2006. Object-oriented land cover classification of LiDAR-derived surfaces. Canadian Journal of Remote Sensing 32(2): 162–172.
16. Yoon, J.-S., Shin, J.-I., Lee, K.-S., 2008. Land cover characteristics of airborne LiDAR intensity data: a case study. IEEE Geoscience and Remote Sensing Letters 5(4): 801–805.
17. Yan, W.Y., Shaker, A., Habib, A., Kersting, A.P., 2012. Improving classification accuracy of airborne LiDAR intensity data by geometric calibration and radiometric correction. ISPRS Journal of Photogrammetry and Remote Sensing 67, 35–44.
18. Yan, W.Y., Shaker, A., 2014. Radiometric correction and normalization of airborne LiDAR intensity data for improving land cover classification. IEEE Transactions on Geoscience and Remote Sensing 52(10): 7658–7673.
19. Im, J., Jensen, J.R., Hodgson, M.E., 2008. Object-based land cover classification using high-posting-density LiDAR data. GIScience & Remote Sensing 45(2): 209–228.
20. Zhou, W., Huang, G., Troy, A., Cadenasso, M., 2009. Object-based land cover classification of shaded areas in high spatial resolution imagery of urban areas: a comparison study. Remote Sensing of Environment 113(8): 1769–1777.
21. MacFaden, S.W., ONeil-Dunne, J.P., Royar, A.R., Lu, J.W., Rundle, A.G., 2012. High-resolution tree canopy mapping for New York City using LiDAR and object-based image analysis. Journal of Applied Remote Sensing 6(1): 063567–1–063567–23.
22. Zhou, W., July 2013. An object-based approach for urban land cover classification: integrating LiDAR height and intensity data. IEEE Geoscience and Remote Sensing Letters 10(4): 928–931.
23. Hecht, R., Meinel, G., Buchroithner, M.F., 2008. Estimation of urban green volume based on single-pulse LiDAR data. IEEE Transactions on Geoscience and Remote Sensing 46(11): 3832–3840.
24. Huang, M., Shyue, S., Lee, L., Kao, C., 2008. A knowledge-based approach to urban feature classification using aerial imagery with LiDAR data. Photogrammetric Engineering & Remote Sensing 74(12): 1473–1485.
25. Guan, H., Ji, Z., Zhong, L., Li, J., Ren, Q., 2013. Partially supervised hierarchical classification for urban features from LiDAR data with aerial imagery. International Journal of Remote Sensing 34(1): 190–210.
26. Chen, Y., Su, W., Li, J., Sun, Z., 2009. Hierarchical object-oriented classification using very high-resolution imagery and LiDAR data over urban areas. Advances in Space Research 43(7): 1101–1110.
27. Antonarakis, A., Richards, K., Brasington, J., 2008. Object-based land cover classification using airborne LiDAR. Remote Sensing of Environment 112(6): 2988–2998.
28. Singh, K.K., Vogler, J.B., Shoemaker, D.A., Meentemeyer, R.K., 2012. Lidar-Landsat data fusion for large-area assessment of urban land cover: balancing spatial resolution, data volume, and mapping accuracy. ISPRS Journal of Photogrammetry and Remote Sensing 74, 110–121.
29. Sasaki, T., Imanishi, J., Ioki, K., Morimoto, Y., Kitada, K., 2012. Object-based classification of land cover and tree species by integrating airborne LiDAR and high spatial resolution imagery data. Landscape and Ecological Engineering 8(2): 157–171.
30. Hartfield, K.A., Landau, K.I., Van Leeuwen, W.J., 2011. Fusion of high resolution aerial multispectral and LiDAR data: land cover in the context of urban mosquito habitat. Remote Sensing 3(11): 2364–2383.
31. Yanjing, J., 2015. Object-based Land Cover Classification with Orthophoto and LIDAR Data. Master of Science Thesis in Geoinformatics TRITA-GIT EX 15-001.